SAND2008-4774C

Mass Sensitive, Lorentz-Force Actuated, MEMS Preconcentrator and Chemical Sensor

Ronald P. Manginell[a], Douglas R. Adkins[b], Matthew W. Moorman[a], Rameen Hadizadeh[c], Davor Copic[c], Daniel Porter[c], John M. Anderson[a], David R. Wheeler[a], Kent B. Pfeifer[a] and Arthur Rumpf[a]

[a] Sandia National Laboratories, Albuquerque, New Mexico 87185, USA
[b] Defiant Technologies, Inc., Albuquerque, New Mexico 87109, USA
[c] University of Louisville, Louisville, Kentucky, 40292 USA

The mass-sensitive smart preconcentrator (SPC) consists of a Lorentz-Force-actuated MEMS resonator with an integral heater and surface coating for the collection of chemical analytes. Control circuitry is used to drive the SPC to resonance and measure its oscillation frequency. The frequency shift produced by adsorption of analyte on the SPC surface is inversely proportional to the mass of analyte collected. Thus, the SPC can measure when it has collected sufficient analyte for a downstream detection system. The limit of detection (LOD) of the SPC is less than 50 ppb for DMMP (dimethyl-methyl-phosphonate). At 1 ppm, less than 1 second collection of DMMP is sufficient to trigger analysis. An analytical model of operation of the SPC is used to predict the motion of the paddle and the shear modulus of silicon.

Introduction

There have been several efforts over the course of the past few decades to develop miniature gas chromatography (GC) based chemical detection systems (1-4). These typically employ a front-end preconcentrator device to capture analytes of interest and boost their concentration into a range detectable by existing sensor technologies. The earliest microfabricated preconcentrators (PC) were planar in design, and despite small relative collection areas, these still work quite well for semivolatile compounds (5-6). High surface area microfabricated PCs were later introduced to improve concentration factors and expand the range of analytes to volatile compounds and explosives (7-12). Voiculescu has recently published a review of micropreconcentrators (13).

This paper describes a novel smart preconcentrator (SPC) that can measure the amount of analyte it has collected. This permits it to determine when it has collected sufficient analyte for detection by a downstream GC-based microanalytical system. It can also be used as a detector in its own right, situated downstream of a microGC and preconcentrator (14).

Operation of the Smart Preconcentrator

The smart preconcentrator (SPC) consists of a rectangular paddle of silicon suspended over an air gap by two torsional tethers, as shown in Figures 1 and 2. An AC current, *i*, is driven through the metal transducer shown on the right side of the paddle. A Lorentz Force is created by the interaction of the current with a transverse, in plane magnetic field,

B, produced by miniature permanent magnets located along the outside perimeter of the die (not shown). Given the nature of the paddle suspension, the Lorentz Force ($F \sim i \cdot B$) creates a torque on the paddle that compels it to rotate about its central symmetry axis. The sign of the torque varies with the phase of the AC current. The resonant frequency can be located by sweeping the AC current frequency. The induced current (i_p) on the transducer line, shown on the left side of the paddle in Fig. 1, is used to measure the oscillation frequency. The SPC has a thin-film adsorbent layer deposited on its surface to collect chemical analytes. As analytes are adsorbed, the mass change of the system is monitored. When the mass change is deemed sufficient, as determined through knowledge of the performance of a downstream detection system, the serpentine heater is pulsed with a square wave voltage to rapidly heat and desorb the collected analyte.

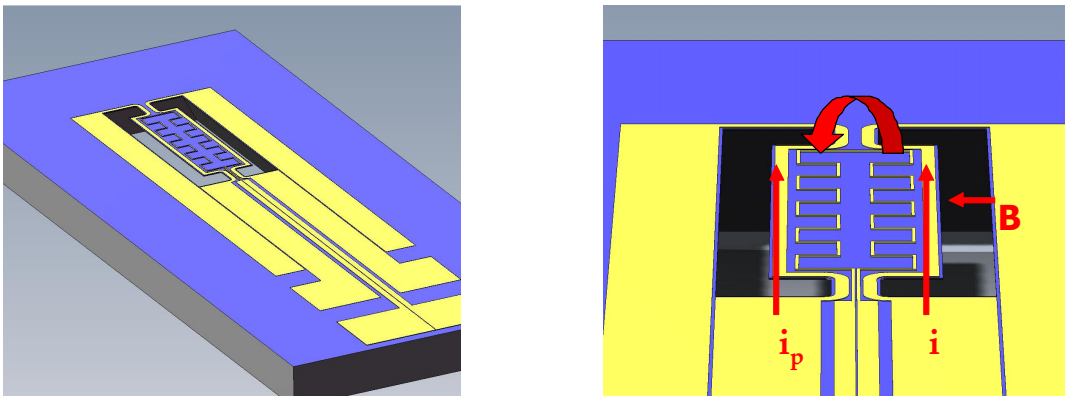

Figure 1. Solid models of the SPC. At left the overall die is shown. At right, a close up of the active area is provided along with an illustration of the rotation created by the Lorentz force.

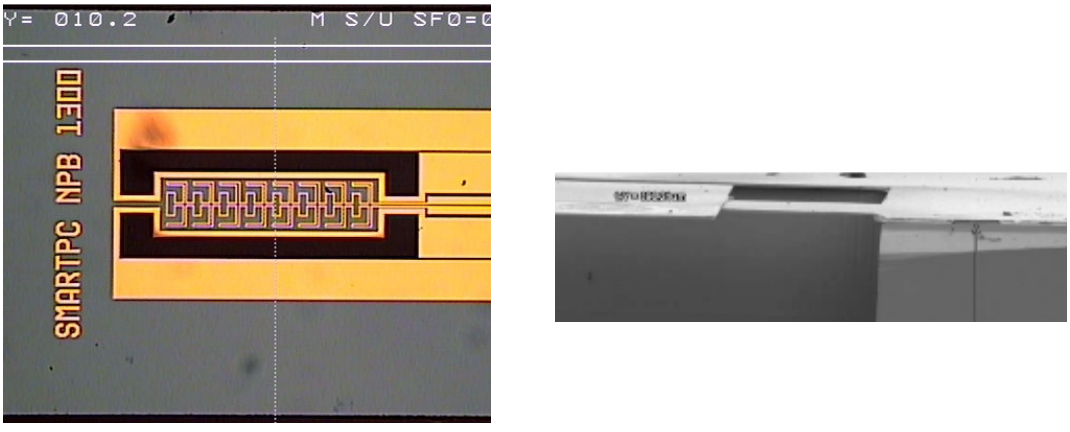

Figure 2. Left: Optical top view of the SPC. Right: SEM perspective view showing one side of the paddle suspended over an air gap by a torsion tether.

Theory

The equation of motion for the SPC is solved elsewhere (15) and summarized here for convenience. The nomenclature used in the model is defined in Table I, below. The moment of inertia and damping constant for the SPC are, respectively,

$$I_m = \rho wcL\left(\frac{c^2 + w^2}{12}\right)$$

$$k = 2\frac{G}{a}bc^3\beta \qquad [1]$$

Table I.: Model Nomenclature

Symbol	Definition	Symbol	Definition	Symbol	Definition
I_m	Inertial Moment	a	Tether Length	γ	Damping Const.
ρ	Paddle Density	b	Tether Width	ω	Frequency [s^{-1}]
c	Paddle Thickness	G	Shear Modulus	ρ_{Si}	Silicon Density
L	Paddle Length	k	Torsion Constant	σ	Adsorbate Surface Density
w	Paddle Width	β	Torsion Parameter	M	Metallization & Adsorbent Mass

The resonant frequency of the SPC is

$$\omega_o = \sqrt{\frac{k}{I_m}} = \sqrt{\frac{24\beta bc^2 G}{\rho wcaL\left(c^2 + w^2\right)}}\ , \qquad [2]$$

where β is a dimensionless torsion parameter that depends on the ratio b/c, and has a limiting value of 1/3 for thin paddles (16). To accommodate the mass of the metal transducers and heaters, and the adsorbent mass, an effective density can be defined

$$\rho = \frac{M + \rho_{Si} wcL}{wcL}\ . \qquad [3]$$

The resonant frequency with an adsorbed analyte of surface density of σ [g/cm^2] is then

$$\omega_n = \sqrt{\frac{24\beta bc^2 G}{\rho waL\left(\rho c + \sigma\right)\left(c^2 + w^2\right)}}\ . \qquad [4]$$

The mass sensitivity of the SPC can be written as

$$S = \frac{\omega_o - \omega_n}{\Delta m}, \qquad [5]$$

where the change in mass with adsorbed analyte has the value

$$\Delta m = \sigma w L \ . \qquad [6]$$

Using equations (2) and (4) the sensitivity becomes

$$S = \frac{\omega_o}{\sigma w L}\left(1 - \sqrt{\frac{\rho c}{\rho c + \sigma}}\right), \qquad [7]$$

which can be simplified to

$$S \cong \frac{\omega_o}{\sigma w L} \qquad [8]$$

for experimentally reasonable values of σ.

Microfabrication and Adsorbent Coating

The microfabrication process is illustrated graphically in Figure 3. Silicon on insulator wafers (SOI) with nominal 5 micron device layer, 1 micron BOX and 400 micron handle are used (Figure 3a). The metal heater and transducer lines are first created by deposition and liftoff patterning (solid black boxes in Figure 3b) over a thin dielectric isolation layer (not shown). Next, two 'u'-shaped patterns are etched through the device layer, stopping on the BOX (buried oxide). Figure 3c provides side and top views of this step. This step defines the planar dimensions of the paddle and torsional beams, while the thickness of the resonator is determined by the device layer thickness. In the last step, Figure 3d, the paddle is undercut by etching through the wafer, from the opposite side to the BOX. Alignment of the etch mask to the front side patterns is achieved using a Karl Suss MA/6 aligner. Both KOH and Bosch etching have been used for the latter etch step, though Figure 3d is indicative of Bosch etching.

Following microfabrication, adsorbent and reference materials are applied to the SPCs using an in-house-developed, ultrasonic-nebulizer-based coating system. Hydrogen-bond acid modified sol gels are used for adsorbents in this work given their

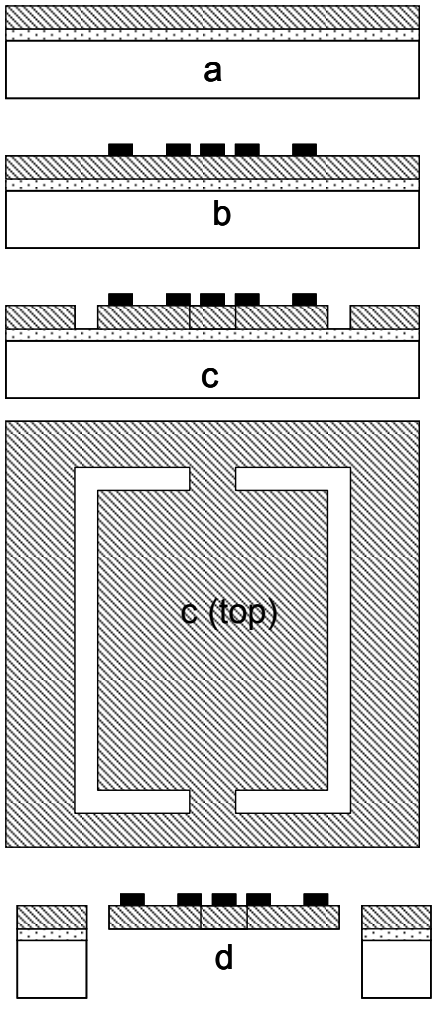

Figure 3. Cross section illustration of the microfabrication sequence.

selectivity towards organophosphonate compounds. Reference devices are passivated by application of an aminosilane treatment to the silicon paddle to reduce non-specific adsorption of organophosphonate analytes (15).

Drive and Sense Circuit

To drive the SPC into oscillation and monitor its response during analyte collection, the circuit of Figure 4 was developed. The circuit is described in detail in (15). Briefly, one of the transducer wires is driven with current *i*. The trans-impedance amplifier (Trans.) produces an output voltage proportional to the pickup current in the other transducer. See Figure 2 to locate the two currents just mentioned. The Trans. voltage is input into a phase-locked loop (PLL) and compared with the PLL's onboard oscillator frequency. The oscillator frequency can be tuned by the digital potentiometer (Dig. Pot), providing computer control of the oscillator frequency. Initially, the circuit is auto tuned using the micro-controller and digital pot to the resonant frequency of the SPC. In subsequent operation, frequency changes brought on by analyte challenges move the circuit off the PLL oscillator frequency and an "error voltage" is produced. The error voltage is therefore proportional to the frequency changes of the SPC with collected analyte. The error voltage is filtered (Filter) and coupled to an A/D converter (ADC). The microcontroller (PIC16C62B) also has the ability to measure the frequency directly via a multiplexed counter circuit implemented on the board. Interface with a host computer is accomplished using RS-232 and a program written in Visual-Basic. The heater portion of the circuit (Heat) is activated by the PIC to rapidly heat the SPC to its desorption temperature once sufficient analyte has been collected.

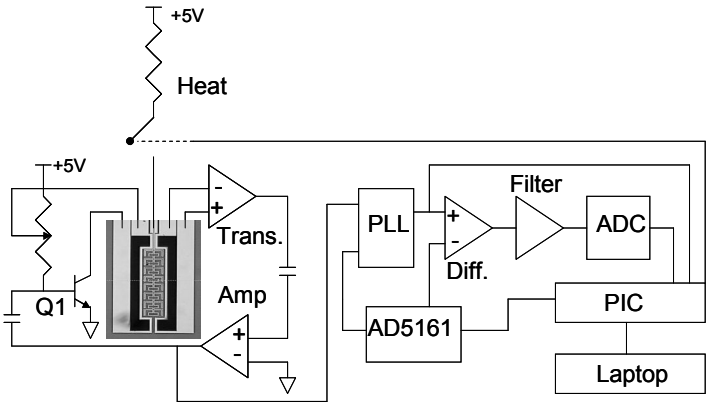

Figure 4. Drive and sense circuit.

Testing and Data

Special packaging was created to house the SPC (Figure 5). The advantage of the approach shown that figure is that simultaneous fluidic sealing and electrical contact to the SPC is made in one simple step. After inserting the die into the package, lids are tightened to the PEEK manifold using standard fasteners, and in a single step, o-ring seals and miniature spring contacts are simultaneously compressed.

A vapor generation system consisting of a temperature-controlled diffusion vial of DMMP (dimethyl-methyl-phosphonate) and a calibrated flow of dilution nitrogen was used to challenge the SPCs with quantifiable amounts of analyte. All flow lines exterior to the temperature-controlled oven were heated in an insulated trunk line to prevent unwanted condensation. The test packages were connected to the output of the vapor system, while the control circuit of Fig. 4 was used for acquiring data.

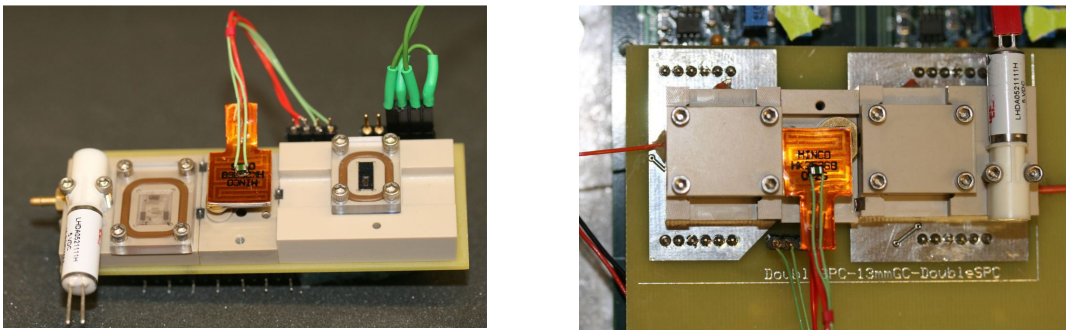

Figure 5. Left: Modular packaging of a minivalve, SAW sensor, microGC with Minco heater, and SPC (from left to right). Right: another rendition with opaque PEEK lids covering the micro components. The package is directly connected to the control circuit.

Raw data is shown in Figure 6 for the response of an SPC to 500 ppbv of DMMP. The trace labeled 'sensor' is for an SPC coated with sol gel. The relatively flat response of the 'reference' device is due to the aminosilane treatment, mentioned above. After an initial precipitous drop, the sensor response tails off until the heater is pulsed to release the collected analyte, and the response begins to return to baseline. The response of the SPC was tested from approximately 150 ppbv – 1 ppmv of DMMP. The time required for two separate devices to obtain a S/N ratio of 3:1 was determined as a function of concentration from this data set; the response times of the two devices were averaged to obtain the response time for the SPC to detect DMMP at a given concentration (15). The collective data shows that as the concentration increases to the lethal limit of sarin, the response time for the SPC to detect DMMP drops to about 0.6 second. With typical preconcentrators an arbitrary collection time, normally set at one minute or greater, would be required. Therefore, the SPC diminishes collection times by a minute or so at high concentrations. Also based on this data, the limit of detection for Sarin was determined to be less than 50 ppbv, the actual value being restricted for disclosure by export control regulations.

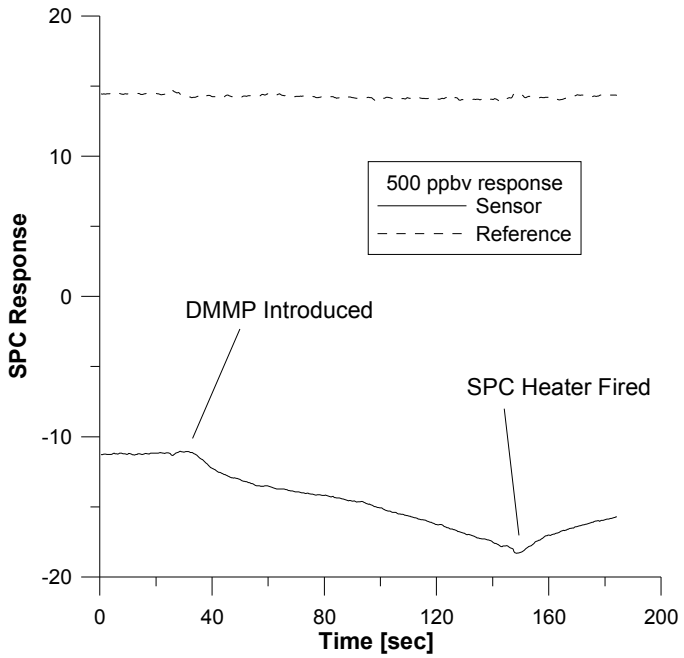

Figure 6. Bare responses of a sol-gel coated sensor SPC and aminosilane passivated reference SPC to 500 ppbv of DMMP. The units on the vertical axis are omitted due to export control limitations.

Design Variations and the Shear Modulus of Si(100)

Five design variations were fabricated to elucidate the variation in sensitivity with the physical dimensions of the SPC. The sensitivity of a given design was determined from the magnitude of its response at a given concentration. The responses for the different designs were normalized to that of the most sensitive design in the column labeled "Ave. Sensitivity" in Table II. The resonant frequency for each design was also measured so that Equation [8] could be used to predict the relative sensitivity of the designs. In all cases, L = 1500 micron, a = 200 micron and c = 5 micron were fixed. The values of β were taken from (16). Based on Equation [2] the shear modulus of silicon (100) was predicted.

Table II. Design variations, sensitivity & the shear modulus of Si(100).

Design	Resonant Frequency (kHz)	Effective Density (g/cm^3)	β	G Predicted (GPa)	Predicted Relative Sensitivity	Ave. Sensitivity
1	19.6	3.38	0.318	56.0	1	1
2	17.0	3.39	0.316	55.0	0.88	.8
3	14.6	3.34	0.317	60	0.60	.56
4	11.9	3.29	0.318	56.0	0.44	-
5	9.8	3.21	0.316	47.5	0.39	-

The average shear modulus of Si (100) from Table II is 54.9 GPa ± 5.5 GPa. Treating the value of 47.5 GPa as an outlier yields an average shear modulus of 57.0 GPa ± 2.2 GPa. With the exception of the results for device 5, the present work predicts a shear modulus of Si (100) that falls in the range reported by Kim (17) of 51 – 79 GPa. "Softening" of the silicon predicted by Evoy (18) and Dowell (19) by an analysis of nanopaddle oscillators is not anticipated by the results of this paper. The average measured sensitivity closely matches the sensitivity predicted by the model.

Conclusions

The SPC can be used as a preconcentrator, or as a sensor in its own right. Given its ability to detect when it has collected sufficient analyte for analysis by a downstream system, the SPC effectively expands the dynamic range of systems in which it is used. Ordinary preconcentrators, macro or micro-sized, require an arbitary collection time, wasting time at high concentrations. The SPC allows analysis times to be shortened drastically when ambient chemical concentrations are greatest and most dangerous to human life. It also prevents overloading of downstream detectors in high-concentration detection scenarios. Systems based on the SPC can have collection cycle times shorter than 1 second with specificity at lethal concentrations. This is comparable, or shorter in duration than IMS-based systems. The existing SPC design has a LOD less than 50 ppb at 3:1 signal to noise. The theory of operation allows for optimization of the SPC sensitivity, is applicable to other torsional oscillators, and can be used in the measurement of the shear modulus of silicon.

Acknowledgments

The authors would like to acknowledge P. R. Lewis, J. M. Bauer, E. Heller, J. Blaich, B. Scherzinger, L. J. Sanchez, B. Norton, J. Dickinson, P. Fletcher, J. Gordon, W. K. Schubert, J. Byrnes, C. Flack, S. Howell, M. Siegal, and T. J. Ross. Sandia is a multiprogram laboratory operated by Sandia Corporation, a Lockheed Martin Company for the United States Department of Energy's National Nuclear Security Administration under contract DE-AC04-94AL85000. The authors would like to acknowledge the financial support Sandia National Laboratories LDRD program.

References

1. S. C. Terry, J. H. Jerman and J. B. Angell, *IEEE Trans. Electron Dev.*, **26**, 1880 (1979).
2. P. R. Lewis, R. P. Manginell, D. R. Adkins, R. J. Kottenstette, D. R. Wheeler, S. S. Sokolowski, D. E. Trudell, J. E. Byrnes, M. Okandan, J. M. Bauer, R. G. Manley, and G. C. Frye-Mason, *IEEE Sensors Journal*, **6**, 784 (2006).
3. C.-J. Lu, W. H. Steinecker, W.-C. Tian, M. C. Oborny, J. M. Nichols, M. Agah, J. A. Potkay, H. K. L. Chan, J. Driscoll, R. D. Sacks, K. D. Wise, S. W. Pang and E. T. Zellers, *Lab Chip*, **5**, 1123 (2005).
4. F. L. Dorman, E. B. Overton, J. J. Whiting, J. W. Cochran, J. Gardea-Torresday, Anal. Chem., **80**, 4487 (2008).

5. R. P. Manginell, G. C. Frye-Mason, R. J. Kottenstette, P. R. Lewis, and C. C. Wong, in *Tech. Digest Sol.-State Sensor and Actuator Workshop*, p. 179, Transducers Research Foundation, (2000).
6. R. P. Manginell, S. Radhakrishnan, M. Shariati, A. L. Robinson, J. A. Ellison, and R. J. Simonson, *IEEE Sensors Journal*, **7**, 1032 (2007).
7. W. C. Tian, H. K. L. Chan, C. J. Lu, S. W. Pang and E. T. Zellers, *Journal of Microelectromechanical Systems*, **14**, 498 (2005).
8. R. P. Manginell, S. Sokolowski, P. R. Lewis, D. R. Adkins, R. J. Kottenstette, M. W. Moorman, S. K. Showalter, R. J. Shul and M. Siegal, Sandia National Laboratories, Albuquerque, USA, SAND2004-6316 (2004).
9. A. M. Ruiz, I. Gracia, N. Sabate, P. Ivanov, A. Sanchez, M. Duch, M. Gerboles, A. Moreno, C. Cane, "Membrane-suspended microgrid as a gas preconcentrator for chromatographic applications," *Sensors and Actuators*, *A*, **135**, 192 (2007).
10. R. A. Veeneman and E. T. Zellers, in *Tech. Digest Sol.-State Sensor and Actuator Workshop*, p. 252, Transducers Research Foundation, (2008).
11. B. Alfeeli, M. Ashraf-Khorassani, L. T. Taylor, and M. Agah, in *Tech. Digest Sol.-State Sensor and Actuator Workshop*, p. 118, Transducers Research Foundation (2008).
12. R. P. Manginell, "Simulation software speeds microfluidics development," *Small Times*, July 17, 2007.
13. I. Voiculescu, M. Zaghloul and N. Narasimhan, *Trends Anal. Chem*., **27**, 327 (2008).
14. R. P. Manginell, M. Okandan, R. J. Kottentstette, P. R. Lewis, D. R. Adkins, R. J. Shul, J. M. Bauer, R. G. Manley and S. Sokolowski, in *Proceedings of the μ-TAS 2003 Workshop*, p. 1247, Transducers Research Foundation (2003).
15. R. P. Manginell, D. R. Adkins, M. W. Moorman, R Hadizadeh, D. Copic, D. Porter, J. M. Anderson, D. R. Wheeler, K. B. Pfeifer and A. Rumpf, in press *J. Microelectromechanical Systems*.
16. H. Ford and J. Alexander, *Advanced Mechanics of Materials, 2nd Ed*. New York: John Wiley & Sons Inc., 1977.
17. J. Kim, D. Cho, and R. S. Muller, in *Transducers 2001 and EuroSensors XV*, **1**, 662 (2001).
18. S. Evoy, D. W. Carr, L. Sekaric, A. Olkhovets, J. M. Parpia and H. G. Craighead, *J. Applied Physics*, **86**, 6072 (1999).
19. E. H. Dowell and D. Tang, *J. App. Phys*., **90**, 5606 (2001).